

Article

Numerical Simulations on Polarization Quantum Noise Squeezing for Ultrashort Solitons in Optical Fiber with Enlarged Mode Field Area

Arseny A. Sorokin ¹, Elena A. Anashkina ^{1,2,*} , Joel F. Corney ³, Vjaceslavs Bobrovs ⁴ , Gerd Leuchs ^{1,5} 
and Alexey V. Andrianov ¹

¹ Institute of Applied Physics of the Russian Academy of Sciences, 46 Ul'yanov Street, 603950 Nizhny Novgorod, Russia; arsorok1997@yandex.ru (A.A.S.); gerd.leuchs@mpl.mpg.de (G.L.); andrian@ipfran.ru (A.V.A.)

² Advanced School of General and Applied Physics, Lobachevsky State University of Nizhny Novgorod, 23 Gagarin Ave., 603950 Nizhny Novgorod, Russia

³ School of Mathematics and Physics, The University of Queensland, Brisbane, Queensland 4072, Australia; corney@physics.uq.edu.au

⁴ Institute of Telecommunications of Riga Technical University, 12 Azenes Street 1, 1048 Riga, Latvia; vjaceslavs.bobrovs@rtu.lv

⁵ Max Planck Institute for the Science of Light, Staudtstr. 2, 91058 Erlangen, Germany

* Correspondence: elena.anashkina@ipfran.ru

Abstract: Broadband quantum noise suppression of light is required for many applications, including detection of gravitational waves, quantum sensing, and quantum communication. Here, using numerical simulations, we investigate the possibility of polarization squeezing of ultrashort soliton pulses in an optical fiber with an enlarged mode field area, such as large-mode area or multicore fibers (to scale up the pulse energy). Our model includes the second-order dispersion, Kerr and Raman effects, quantum noise, and optical losses. In simulations, we switch on and switch off Raman effects and losses to find their contribution to squeezing of optical pulses with different durations (0.1–1 ps). For longer solitons, the peak power is lower and a longer fiber is required to attain the same squeezing as for shorter solitons, when Raman effects and losses are neglected. In the full model, we demonstrate optimal pulse duration (~0.4 ps) since losses limit squeezing of longer pulses and Raman effects limit squeezing of shorter pulses.

Keywords: polarization squeezing; quantum noise suppression; stochastic nonlinear Schrödinger equation; optical soliton; nonlinear fiber optics



Citation: Sorokin, A.A.; Anashkina, E.A.; Corney, J.F.; Bobrovs, V.; Leuchs, G.; Andrianov, A.V. Numerical Simulations on Polarization Quantum Noise Squeezing for Ultrashort Solitons in Optical Fiber with Enlarged Mode Field Area. *Photonics* **2021**, *8*, 226. <https://doi.org/10.3390/photonics8060226>

Received: 14 May 2021

Accepted: 15 June 2021

Published: 18 June 2021

Publisher's Note: MDPI stays neutral with regard to jurisdictional claims in published maps and institutional affiliations.



Copyright: © 2021 by the authors. Licensee MDPI, Basel, Switzerland. This article is an open access article distributed under the terms and conditions of the Creative Commons Attribution (CC BY) license (<https://creativecommons.org/licenses/by/4.0/>).

1. Introduction

Broadband quantum noise suppression of light is desirable for many applications, including detection of gravitational waves, quantum sensing, and quantum communication [1]. For example, the first long-term application of quantum squeezed light for a gravitational-wave observatory was reported in [2]. In new detectors of gravitational waves, an injection of –10 dB squeezed light is required and studies in this direction are in progress [3]. With regard to quantum communications, the first implementation of an entirely guided-wave optical setup for generation and detection of squeezed light at a telecommunication wavelength was reported in [4]. Thus, the development and investigation of methods for quantum noise suppression is of interest for many applications. When studying optical pulses in fibers, quasi-particle excitations called solitons play a special role in the spectral region of anomalous dispersion because of their remarkable stability [5–7]. The underlying reason for this is the compensation of dispersion by the Kerr nonlinear interaction in the medium. In classical optics, such solitons have a well-defined phase and amplitude. When characterizing the light with high enough precision, one discovers

that amplitude and phase are subject to some quantum uncertainty. This uncertainty is minimized e.g., for the coherent state. As a result, a quantum soliton in a coherent state will not be stable, but will instead show a quantum evolution, which in the case of an optical fiber is typically dominated by the Kerr-effect [8]. Only if the bright soliton with a high mean photon number is in a well-defined photon number (Fock) state will it be stationary, but this is an unrealistic scenario for solitons in fibers. However, the quantum evolution of an initially coherent soliton generates a soliton in a squeezed state, showing reduced quantum noise, which can be useful. Interfering two squeezed solitons generates entangled solitons with potential use in interferometry and communication (see e.g., [9]). Incidentally, the initial part of the quantum evolution of a coherent state, continuous wave (CW) or pulsed, and that of the classical evolution of a light field with statistical fluctuations corresponding the same quantum uncertainty, are very similar [10–12]. However, the later evolution is much different because the quantum evolution is ultimately periodic [13,14], in stark contrast to classical evolution. Recently it was pointed out that entangled light beams may improve the sensitivity of ellipsometry [15], which is not surprising, because ellipsometry is also a form of interferometry.

There are several ways to obtain (CW) or pulsed squeezed light (see the review [1] and references therein). This can be done, for example, by means of semiconductor lasers [16], parametric down-conversion [17], optical parametric systems [17,18], parametric up-conversion [19–21], and optical fibers with a Kerr nonlinearity [22,23]. The first demonstration of quantum squeezing in an optical fiber was reported in [22]. Soliton squeezing of -2.7 dB (-4 dB with correction of detection losses) was achieved in a microstructured fiber [24]. A maximum noise reduction of 4.4 dB (6.3 dB with correction for losses) was obtained for ultrashort pulses in a polarization-maintaining fiber [25]. Polarization squeezing of -6.8 dB (-10.4 dB with corrected for linear losses) of ultrashort pulses in a birefringent fiber was presented in [26]. However, the potential for optical fibers is not yet fully exploited, and possibilities of efficient noise reduction in fibers are studied [27–29]. In most experiments on Kerr squeezing, fibers with high nonlinear coefficients were used [23–26]. Note that in optical fibers, the nonlinear Kerr coefficient γ is proportional to the nonlinear refractive index n_2 , which is an intrinsic material property, and is inversely proportional to the effective mode field area A_{eff} , which depends on fiber design and can be controlled in a wide range [30]. Here we consider a silica fiber with an enlarged A_{eff} compared to standard telecommunication fibers and expect that such a fiber with a reduced nonlinear coefficient of γ may be useful for operation with higher peak powers and higher pulse energies. In addition, it was recently shown that using fibers with large A_{eff} allows for mitigating guided acoustic wave Brillouin scattering (GAWBS), which is a parasitic effect for the squeezing of light [31].

Squeezing of CW and pulsed light in fibers has its own advantages and limiting factors. For Kerr squeezing of narrowband CW radiation, long fibers (~ 100 m) are required, and optical losses as well as GAWBS [32] are limiting factors. For ultrashort soliton pulses with a high peak power and a broadband spectrum, shorter fibers are required (~ 10 m for pulse duration of the order of 100 fs), therefore the impact of losses and GAWBS weakens. However, in this case, Raman effects reduce squeezing significantly [26]. A possible way to overcome this limitation is to use longer pulses. However, the soliton energy is inversely proportional to the soliton duration and in standard or highly nonlinear fibers is low for longer pulses. To scale up the soliton energy, fibers with lower nonlinearity can be used. Such fibers are available in the form of large-mode-area (LMA) fibers and multicore coupled-core fibers supporting supermode propagation with a large effective area [30].

Here, we numerically simulate polarization squeezing of ultrashort solitons in fibers with an enlarged mode field area and reduced nonlinearity and study the interplay between limiting factors for different pulse durations. We find optimal conditions and expected quantum noise reduction for them.

2. Methods

Here, we consider a polarization squeezing of optical solitons in a silica fiber with enlarged mode field area and with the decreased nonlinear Kerr coefficient γ compared to a standard telecom fiber SMF-28e ($A_{\text{eff}} \sim 80 \mu\text{m}^2$ for SMF-28e). Current technologies make it possible to produce low-loss fibers with different designs including (i) with a small difference between the refractive indices of cladding and an increased core (LMA fibers) [30] or (ii) multicore fibers with N coupled cores with a standard diameter [30,33] (also studied for quantum telecommunications [34]), for which field area of a stable supermode is approximately N times larger than for a one-core fiber [35,36].

For LMA and multicore fibers, the group velocity dispersion can be similar to the dispersion of silica glass [30]. The refractive index of the silica glass is given in [30]. For SMF-28e, optical loss is ~ 0.2 dB/km in the $1.5 \mu\text{m}$ range [30], but here we take a 5 times higher loss value of α since additional losses may arise when drawing a non-standard fiber. We study squeezing of optical solitons with a full width at half maximum (FWHM) duration of $T_{\text{FWHM}} = 0.1\text{--}1$ ps at a central wavelength λ_0 in the telecom range at room temperature T . Simulation parameters are given in Table 1.

Table 1. Parameters used in the simulation.

Parameter	Value
β_2	$-28.0 \text{ ps}^2/\text{km}$
A_{eff}	$960 \mu\text{m}^2$
γ	$0.093 (\text{W}\cdot\text{km})^{-1}$
α	$1.0 \text{ dB}/\text{km}$
λ_0	$1.5 \mu\text{m}$
T	300 K

We consider the system for polarization squeezing of ultrashort optical pulses as presented in [23], since it is one of the most experimentally stable techniques to obtain Kerr squeezing. The system is based on the propagation of two pulses with the orthogonal polarizations aligned along axes of a birefringent fiber. Note that birefringent LMA and multicore fibers can be produced with current technologies. Polarization-maintaining photonic crystal LMA fibers and solid-core LMA fibers are commonly used in high-power laser systems and are commercially available [37]. Their birefringent properties arise from anisotropic stress induced by special structures or from asymmetric (e.g., elliptical) core shape. Multicore birefringent fibers can also be made utilizing similar technologies. For example, 98-core fiber with stress-applying rods placed near each of the cores was demonstrated in [38], and 5-core micro-structured multicore fiber was demonstrated in [39]. Usually the pulses are launched into the birefringent fiber with some delay to compensate for group velocities difference, such that they arrive at the output at the same time. The polarization state of the output signal has quantum uncertainty. However, the uncertainty along some directions in the Poincare sphere can be lowered at the expense of an increase in uncertainty in the other directions, and thus, the polarization squeezing is obtained. Due to propagation of both pulses in the same fiber, technical and acoustical noise associated with the fiber is almost canceled out. Polarization squeezing is useful for increasing the precision of polarimetry [15] and for broader class of interferometric measurements in which the quantity to be measured is mapped onto the polarization state.

The transformation of the noise statistics occurs during the propagation of the pulses in the fiber under the action of a Kerr nonlinearity. Hence, the most computationally intensive part is the simulation of the pulse propagation with an allowance for quantum noise. Some assumptions are made to simplify numerical modeling. First, we consider the propagation of orthogonally polarized pulses to be almost independent. Next, we use a truncated Wigner technique for modeling pulse propagation, which provides accurate results for relatively short propagation distances and a large photon number. We perform scalar modeling based on the Raman-modified stochastic nonlinear Schrödinger equation [40–42]

with an allowance for losses of the signals in both polarizations, and combine the output results to calculate the polarization squeezing at the last step.

The slowly varying electric field envelope $A_{sol}(z, t)$ of a linearly polarized fundamental optical soliton propagating in a fiber with a Kerr nonlinearity, and the second-order dispersion β_2 neglecting other effects in the framework of a *classical* nonlinear Schrödinger equation is [30,43]:

$$A_{sol}(t, z) = \frac{\sqrt{P_0} \exp[iz/(2L_D)]}{\cosh(t/t_0)}, \tag{1}$$

where z is a coordinate along fiber, t is time in the retarded frame, $L_D = t_0^2/\beta_2$ is the dispersion length, t_0 is related to T_{FWHM} as $T_{FWHM} = 2\ln(1 + 2^{1/2})t_0 \approx 1.763t_0$ [30]. For a fundamental soliton, the peak power P_0 is inversely proportional to the square of its duration [30]:

$$P_0 = \frac{|\beta_2|}{\gamma t_0^2}. \tag{2}$$

To simulate the pulse evolution with allowance for the quantum noise using the Wigner representation, we use the Raman-modified stochastic nonlinear Schrödinger equation [40–42]:

$$\frac{\partial}{\partial z} A(t, z) = i\frac{\beta_2}{2} \frac{\partial^2}{\partial t^2} A(t, z) + \left[i\gamma \int_0^\infty dt' R(t-t') |A(t', z)|^2 + \Gamma^R(t, z) \right] A(t, z) - \alpha A(t, z) + \Gamma(t, z). \tag{3}$$

To perform *quantum dynamical simulations* for the slowly varying envelope of an ultrashort optical pulse $A(z, t)$, we take as the initial condition a fundamental classical soliton $A_{sol}(0, t)$ with an addition of normally distributed stochastic noise $\delta A(0, t)$

$$A(t, 0) = A_{sol}(t, 0) + \delta A(t, 0), \tag{4}$$

$$\langle \delta A(t, 0) \delta A^*(t', 0) \rangle = \frac{\hbar\omega_0}{2} \delta(t - t'). \tag{5}$$

The function $R(t - t')$ describes deterministic nonlinear response including Kerr and Raman contributions, Γ and Γ^R describe linear quantum noise and Raman noise, respectively, while GAWBS is neglected. Note that in the recent work [31], the authors demonstrated that GAWBS influence scales down with increasing effective mode field area A_{eff} , which is the advantage of considered fibers with enlarged A_{eff} and allows us to neglect GAWBS here. Γ and Γ^R are zero-mean delta-correlated random values with normal distribution in the frequency domain

$$\Gamma(\omega, z) = \frac{1}{\sqrt{2\pi}} \int_{-\infty}^\infty \Gamma(t, z) e^{i\omega t} dt, \tag{6}$$

$$\Gamma^R(\omega, z) = \frac{1}{\sqrt{2\pi}} \int_{-\infty}^\infty \Gamma^R(t, z) e^{i\omega t} dt, \tag{7}$$

$$\langle \Gamma(\omega, z) \Gamma^*(\omega', z') \rangle = \alpha \hbar\omega_0 \delta(\omega - \omega') \delta(z - z'), \tag{8}$$

$$\langle \Gamma^R(\omega, z) \Gamma^{R*}(\omega', z') \rangle = \gamma \hbar\omega_0 \alpha^R(\omega) \left(\frac{1}{2} + \frac{1}{\exp\left(\frac{\hbar|\omega|}{kT}\right) - 1} \right) \delta(\omega - \omega') \delta(z - z'), \tag{9}$$

$$\alpha^R(\omega) = 2 \left| \text{Im} \left(\int_0^\infty R(t) e^{i\omega t} dt \right) \right|. \tag{10}$$

In these equations, ω is the angular frequency counted from the central frequency ω_0 , \hbar is the Planck constant, k is the Boltzmann constant. To approximate the experimental Raman gain [44], we use 10-Lorentz fitting with fit parameters F_i, D_i, ω_i for the Raman function [41]:

$$R(t) = (1 - f_R)\delta(t) + f_R \sum_{i=1}^{10} F_i D_i \sin(\omega_i t) e^{-D_i t}, \tag{11}$$

We take $f_R = 0.2$ and the values for the parameters of the Raman function which are given in Table 2. Note that the commonly used Raman function $R_0(t)$ (with only two parameters $\tau_1 = 12.2$ fs and $\tau_2 = 32$ fs) is rather simpler [30]:

$$R_0(t) = (1 - f_R)\delta(t) + f_R(\tau_1^{-2} + \tau_2^{-2})\tau_1 \exp(-t/\tau_2) \sin(t/\tau_1). \tag{12}$$

Table 2. Parameters for the Raman function used in the simulation.

i	F_i	$\omega_i, \text{THz}\cdot\text{rad.}$	$D_i, \text{THz}\cdot\text{rad.}$
1	-0.3545	0.3341	8.0078
2	1.2874	26.1129	46.6540
3	-1.4763	32.7138	33.0592
4	1.0422	40.4917	30.2293
5	-0.4520	45.4704	23.6997
6	0.1623	93.0111	2.1382
7	1.3446	99.1746	26.7883
8	-0.8401	100.274	13.8984
9	-0.5613	114.6250	33.9373
10	0.0906	151.4672	8.3649

Here we take the complicated form of the Raman function $R(t)$ instead of the common form $R_0(t)$ due to 10-Lorenz approximation is more precise at low frequencies. This is important both for accurate soliton evolution and for noise modeling. The imaginary and real parts of spectra of Raman functions $R(t)$ and $R_0(t)$ are also plotted in Figure 1a,b, respectively.

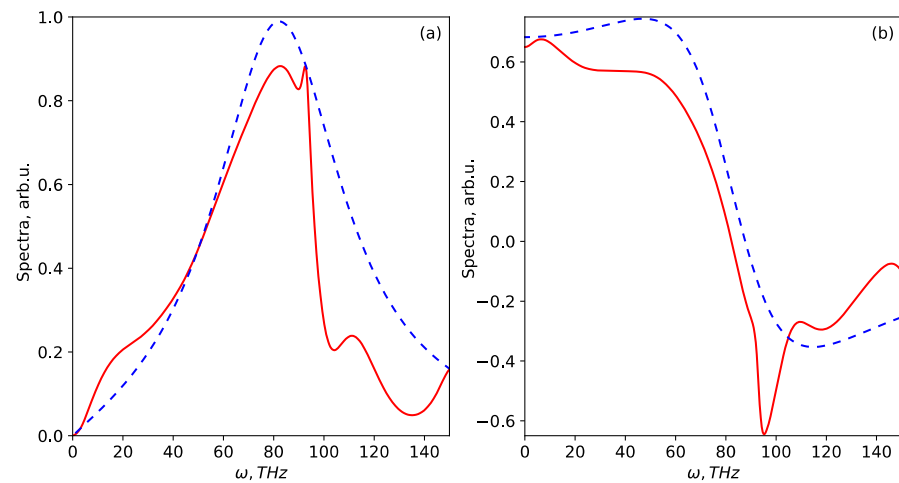


Figure 1. The comparison between the imaginary (a) and real (b) parts of spectra of Raman function $R_0(t)$ given by expression (12) (dashed blue lines) and the Raman function $R(t)$ used in the modeling given by expression (11) (solid red lines).

We find numerical solution of Equation (3) using a specially developed computer code based on the split-step Fourier method [30]. An independent random noise for each realization is added to the initial soliton at $z = 0$.

We modeled the propagation of 1000 independent pairs of x- and y- polarized pulses through a certain fiber length. Then we analyzed the squeezing of polarization uncertainty at the output. We assumed that the detection scheme follows one considered in [23]. In such system, the phases between the orthogonal pulses are set in such a way that the signal at the output has mean circular polarization. Quantum noise introduces uncertainty in the polarization state, so in each individual realization the polarization state is slightly deviate from circular. To characterize the polarization state we calculate integral Stokes

parameters in the Wigner representation, $S_0, S_1, S_2,$ and $S_3,$ analogous to their classical counterparts [23]:

$$S_0(z) = \int dt (A_x^*(t,z)A_x(t,z) + A_y^*(t,z)A_y(t,z)), \tag{13}$$

$$S_1(z) = \int dt (A_x^*(t,z)A_x(t,z) - A_y^*(t,z)A_y(t,z)), \tag{14}$$

$$S_2(z) = \int dt (A_x^*(t,z)A_y(t,z) + A_y^*(t,z)A_x(t,z)), \tag{15}$$

$$S_3(z) = i \int dt (A_y^*(t,z)A_x(t,z) - A_x^*(t,z)A_y(t,z)). \tag{16}$$

It is instructive to plot the set of points representing the polarization state on the plane $S_1 S_2$. In the absence of nonlinearity these points form a symmetric distribution with the uncertainty representing standard quantum limit (see Figure 2a). However, after a nonlinear propagation, the distribution is an ellipse-like cloud (see Figure 2b) with uncertainty in some directions below the standard quantum limit, which represents quantum noise squeezing. We find a minor axis for this cloud and calculate the reduction of noise compared to the initial quantum noise (illustration of the initial cloud and the squeezed cloud is given in Figure 2). We find the angle θ for which the expression for variance V (in dB) is minimal:

$$V = 10 \cdot \log_{10} \left(\frac{\left(\frac{1}{\hbar\omega_0}\right)^2 \langle (S_1 \cos(\theta) + S_2 \sin(\theta))^2 \rangle - \left(\frac{1}{\hbar\omega_0}\right)^2 \langle (S_1 \cos(\theta) + S_2 \sin(\theta)) \rangle^2 - \frac{M}{2}}{\left(\frac{1}{\hbar\omega_0}\right) \langle S_0 \rangle - M} \right). \tag{17}$$

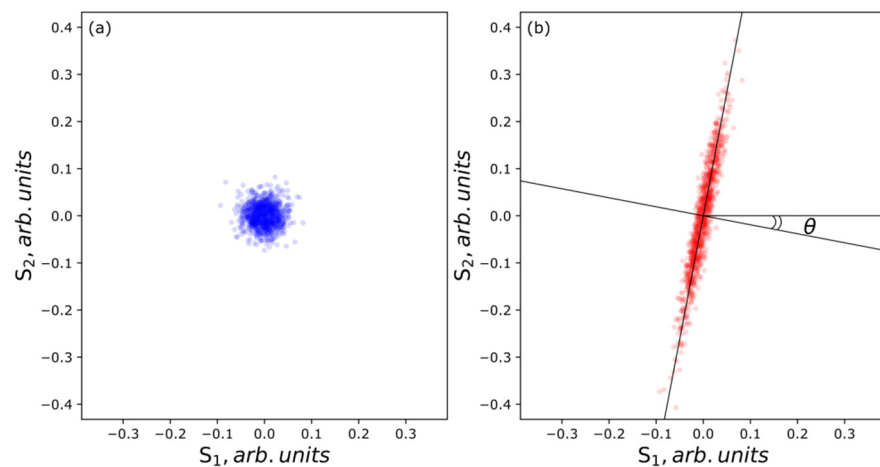


Figure 2. The initial quantum noise cloud (a) and the squeezed quantum noise cloud (b).

In the above equation, the average is taken over the set of realizations, and M is the number of modes used in modeling [23]. Note that for squeezed light V [in dB] $< 0,$ the strongest squeezing is achieved when V is minimal (or, when the absolute value $|V|$ is maximal, which is the same).

We study the influence of Raman effects and linear losses on the squeezing of ultrashort solitons with different durations. For comparison, we also estimate squeezing for CW signals with the equivalent peak powers, which is given under the lossless approximation by the following analytical expression [45]:

$$V_0 = 10 \cdot \log_{10} (1 - 2r_{Kerr} \sqrt{1 + r_{Kerr}^2 + 2r_{Kerr}^2}), \tag{18}$$

here r_{Kerr} is the Kerr parameter $r_{Kerr} = \gamma P_0 \cdot z.$

It is known that if the squeezed light propagates through an element with a loss coefficient $R = 1 - 10^{-\chi/10}$, where χ is a lumped loss in dB, squeezing is reduced to [45,46]:

$$V_{loss} = 10 \cdot \log_{10}[(1 - R)10^{V/10} + R]. \quad (19)$$

We also use Equation (19) for further estimations.

3. Results

First, we performed detailed numerical simulations for solitons with T_{FWHM} durations of 0.2, 0.5, and 1 ps with energies of 5.3, 2.1, and 1.1 nJ, respectively. Their spectral widths ω_{FWHM} are 17.6, 7.1, and 3.5 THz since for a fundamental soliton time–bandwidth product is $T_{FWHM} \cdot \omega_{FWHM} = (8/\pi) \cdot [\ln(1 + 2^{1/2})]^2$ [30]. Raman effects and losses were switched on and switched off to find their contributions to squeezing of pulses with different durations. The simulated results are presented in Figure 3a–f, where the upper and lower rows correspond to modeling without and with Raman effects, respectively. Moreover, for comparison, we evaluated squeezing V_0 of CW signal with the peak powers defined by expression (2) using analytical Formula (18) and evaluated squeezing V_{loss} with allowance for lumped loss $\chi = \alpha \cdot z$ at the fiber output using Formula (19). To study the influence of losses on squeezing of ultrashort pulses, we performed the following series of numerical experiments. We modeled Equation (3) (i) with allowance for distributed losses α , (ii) without any losses, and (iii) without distributed losses but with lumped losses at the fiber output $\chi = \alpha \cdot z$ taken into account using Formula (19).

Here, we analyze the results of modeling when Raman effects are switched off (Figure 3a–c). The loss influence on optimal squeezing is stronger for longer pulses than for shorter pulses. Solitons with longer duration have lower peak power according to expression (2), so for them the significant Kerr parameter r_{Kerr} is accumulated at longer fiber lengths compared to shorter solitons with higher peak power. To attain optimal squeezing, fiber lengths should be longer, and in this case, the loss influence is stronger. The comparison between a simple approximation of losses lumped at the fiber output and modeling with losses distributed along the fiber shows that approximation predicts lower absolute values of optimal squeezing. This may be explained in the following way: the effect of distributed losses along with simple gradual reduction of the pulse energy manifests itself in addition of some vacuum noise along the propagation distance. The noise added at the initial propagation stage gets squeezed in the subsequent fiber pieces. In contrast, approximation given by (19) applies the effect of losses at the output, so that it is not affected by nonlinear propagation.

Next, we analyze the results of modeling when Raman effects are switched on (Figure 3d–f). Here squeezing of the shortest 0.2 ps pulses is drastically decreased, while squeezing of longer pulses is only slightly affected. This is the consequence of smaller overlap of the narrower spectrum of longer pulses with the spectrum of the Raman response function. For 0.2-ps solitons, the Raman effects dominate over the effect of losses, so squeezing curves with and without losses almost coincide in Figure 3d. In contrast, the results for 0.5 ps and 1 ps pulses obtained with Raman effects taken into account presented in Figure 3e are very similar, respectively, to the results obtained without Raman effects presented in Figure 3b,c (compare the corresponding curves in Figure 3b,e as well as in Figure 3c,f).

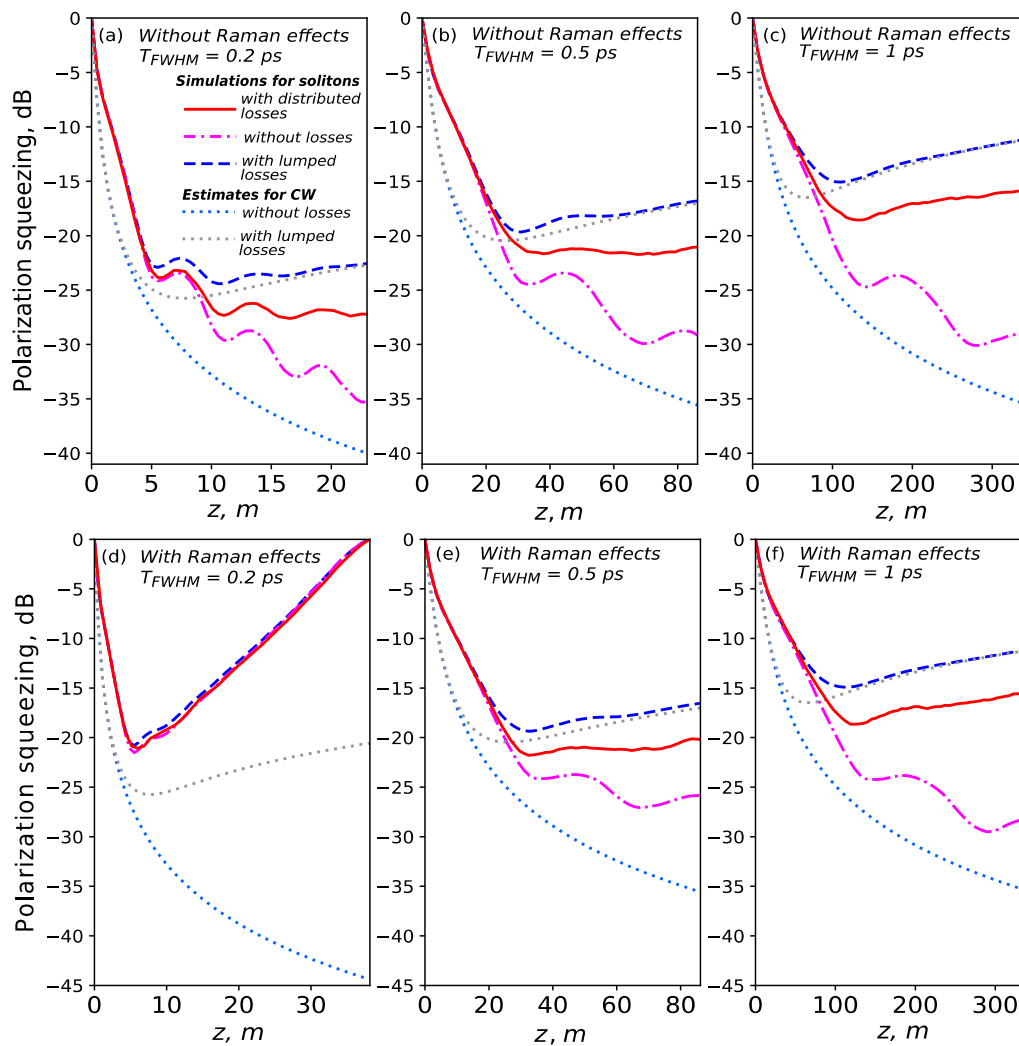


Figure 3. Polarization squeezing simulated without Raman effects for pulse durations of 0.2 ps (a), 0.5 ps (b), and for 1 ps (c) and with full Raman contribution for pulse durations of 0.2 ps (d), 0.5 ps (e), and for 1 ps (f) compared to analytical estimates for squeezing of CW light using Formulas (18) and (19). The legend given in subplot (a) is the same for all subplots. Solid red lines correspond to simulations of Equation (3) with distributed losses; dashed-dotted magenta lines correspond to simulations of Equation (3) without any losses; dashed blue lines correspond to simulations of Equation (3) without distributed losses but with lumped losses; dotted light-blue and gray lines correspond to analytical estimates of squeezing of CW light without losses and with lumped losses, respectively.

Simulations show that optimal fiber lengths are: <10 m for 0.2 ps solitons, a few tens of meters for 0.5 ps solitons, and >100 m for 1 ps solitons. The intermediate soliton durations are preferable to achieve the strongest squeezing (better than -20 dB), since for them the balance between limiting factors (losses for long pulses and Raman effects for short pulses) is satisfied.

Furthermore, we performed simulations for soliton durations in the 0.1–1 ps range with a step of 0.1 ps using full model to find optimal parameters. The optimal (strongest) squeezing and corresponding fiber lengths are demonstrated in Figure 4a,b, respectively. Optimal squeezing of about -22 dB is attained for 0.4 ps solitons with an energy of 2.7 nJ at a fiber length of 23 m.

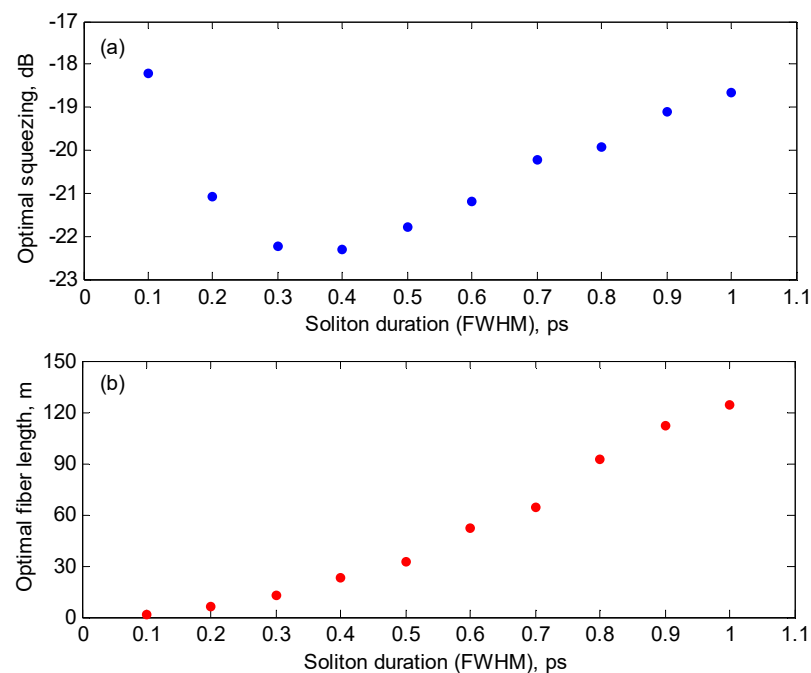


Figure 4. Optimal squeezing (a) and corresponding optimal fiber length (b) as functions of soliton duration.

4. Discussion

We have investigated numerically polarization squeezing of ultrashort solitons with different durations in a silica fiber with enlarged mode field areas such as LMA or multicore fiber (A_{eff} is larger more than ten times compared to the standard telecom fiber SMF28) using realistic parameters in the framework of the Raman-modified stochastic nonlinear Schrödinger equation. Using such fibers allows operating with higher energies compared to the case of SMF28 fiber because soliton energy is inversely proportional to γ (proportional to A_{eff}). Moreover, GAWBS may worsen the quantum noise squeezing for SMF28, since it is inversely proportional to A_{eff} [31].

We have demonstrated that for relatively long solitons ($T_{\text{FWHM}} \geq 0.5$ ps), optical losses limiting squeezing and Raman effects are insignificant. Longer solitons have lower peak powers according to expression (2), and thus for them, longer fiber lengths are required to attain optimal noise suppression in comparison with shorter solitons with higher peak powers. The found optimal fiber lengths are: <10 m for 0.2 ps solitons, a few tens of meters for 0.5 ps solitons, and >100 m for 1 ps solitons. For short solitons ($T_{\text{FWHM}} \leq 0.2$ ps) the Raman effects limit squeezing, which also agrees qualitatively in its functional behavior with prior art experimental results [26,47]. Thus, there is an optimal soliton duration ($T_{\text{FWHM}} \sim 0.4$ ps) when the balance between these limiting factors is satisfied and the strongest squeezing is better than -22 dB.

One observation is that the degree of squeezing oscillates as a function of pulse energy in certain parameter ranges (Figure 3a–c,e,f, dash-dotted magenta lines). The prior experiments in standard fibers show a similar signature. Such studies have also been done for light pulses in micro-structured fibers allowing for tuning the waveguide contribution to dispersion and performing similar experiments in the visible range of the spectrum [48]. Fiorentino et al. [24] have measured the degree of squeezing as a function of pulse energy in a micro-structured fiber. The experimental curve they present also shows slight oscillations. However, the origin of this oscillation does not seem to be clear and requires further studies.

Note that analytical expressions (18) and (19) are very useful for approximate estimates of optimal squeezing of solitons with a duration ≥ 0.5 ps at fiber lengths near optimal values and longer. The analytical formulas for CW light may be used to roughly find an area of parameters for numerical simulation. For solitons with a duration ≤ 0.2 ps,

analytical estimates do not give a reasonable answer since the contribution of Raman effects are dominant.

5. Conclusions

We investigated numerically polarization quantum noise squeezing for ultrashort solitons with 0.1–1 ps durations in a silica fiber with enlarged mode field area. We showed that for relatively long solitons ($T_{FWHM} \geq 0.5$ ps), optical losses limit squeezing and Raman effects are insignificant. For short solitons ($T_{FWHM} \leq 0.2$ ps), the Raman effects limit squeezing. We found that there is an optimal soliton duration ($T_{FWHM} \sim 0.4$ ps) providing the strongest squeezing, better than -22 dB when the balance between limiting factors is satisfied.

Author Contributions: Conceptualization, E.A.A., J.F.C., G.L. and A.V.A.; methodology, A.A.S., J.F.C. and V.B.; software, A.A.S.; formal analysis, A.A.S.; investigation, A.A.S., E.A.A., J.F.C., V.B. and A.V.A.; data curation, A.A.S.; writing—original draft preparation, A.A.S. and E.A.A.; writing—review and editing, J.F.C., V.B., G.L., and A.V.A.; visualization, A.A.S. and E.A.A.; project administration, A.V.A.; funding acquisition, G.L. and A.V.A. All authors have read and agreed to the published version of the manuscript.

Funding: This research was funded in part by Russian Foundation for Basic Research, Grant No. 19-29-11032 (Numerical simulations of squeezing of ultrashort pulses) and in part by the Mega-grant of the Ministry of Science and Higher Education of the Russian Federation, Contract No.14.W03.31.0032 (Analytical estimates of quantum noise suppression of CW light).

Institutional Review Board Statement: Not applicable.

Informed Consent Statement: Not applicable.

Data Availability Statement: Not applicable.

Conflicts of Interest: The authors declare no conflict of interest.

References

1. Andersen, U.L.; Gehring, T.; Marquardt, C.; Leuchs, G. 30 years of squeezed light generation. *Phys. Scr.* **2016**, *91*, 053001. [[CrossRef](#)]
2. Grote, H.; Danzmann, K.; Dooley, K.L.; Schnabel, R.; Slutsky, J.; Vahlbruch, H. First long-term application of squeezed states of light in a gravitational-wave observatory. *Phys. Rev. Lett.* **2013**, *110*, 181101. [[CrossRef](#)]
3. Mansell, G.L.; McRae, T.G.; Altin, P.A.; Yap, M.J.; Ward, R.L.; Slagmolen, B.J.J.; Shaddock, D.A.; McClelland, D.E. Observation of Squeezed Light in the 2 μ m Region. *Phys. Rev. Lett.* **2018**, *120*, 203603. [[CrossRef](#)]
4. Kaiser, F.; Fedrici, B.; Zavatta, A.; d'Auria, V.; Tanzilli, S. A fully guided-wave squeezing experiment for fiber quantum networks. *Optica* **2016**, *3*, 362–365. [[CrossRef](#)]
5. Hasegawa, A.; Tappert, F. Transmission of stationary nonlinear optical pulses in dispersive dielectric fibers. I. Anomalous dispersion. *Appl. Phys. Lett.* **1973**, *23*, 142–144. [[CrossRef](#)]
6. Mitschke, F.M.; Mollenauer, L.F. Discovery of the soliton self-frequency shift. *Opt. Lett.* **1986**, *11*, 659–661. [[CrossRef](#)] [[PubMed](#)]
7. Boutabba, N.; Eleuch, H.; Bouchriha, H. Thermal bath effect on soliton propagation in three-level atomic system. *Synth. Met.* **2009**, *159*, 1239–1243. [[CrossRef](#)]
8. Drummond, P.D.; Shelby, R.M.; Friberg, S.R.; Yamamoto, Y. Quantum solitons in optical fibres. *Nature* **1993**, *365*, 307–313. [[CrossRef](#)]
9. Leuchs, G.; Korolkova, N.V. Entangling Fiber Solitons: Quantum Noise Engineering for Interferometry and Communication. *Opt. Photonics News* **2002**, *13*, 64–69. [[CrossRef](#)]
10. Ritze, H.-H.; Bandilla, A. Quantum effects of a nonlinear interferometer with a Kerr cell. *Opt. Commun.* **1979**, *29*, 126–130. [[CrossRef](#)]
11. Imoto, N.; Haus, H.A.; Yamamoto, Y. Quantum nondemolition measurement of the photon number via the optical Kerr effect. *Phys. Rev. A* **1985**, *32*, 2287–2292. [[CrossRef](#)] [[PubMed](#)]
12. Kitagawa, M.; Yamamoto, Y. Number-phase minimum-uncertainty state with reduced number uncertainty in a Kerr nonlinear interferometer. *Phys. Rev. A* **1986**, *34*, 3974–3988. [[CrossRef](#)]
13. Milburn, G.J. Quantum and classical Liouville dynamics of the anharmonic oscillator. *Phys. Rev. A* **1986**, *33*, 674–685. [[CrossRef](#)]
14. Stobinska, M.; Milburn, G.J.; Wodkiewicz, K. Wigner function evolution of quantum states in the presence of self-Kerr interaction. *Phys. Rev. A* **2008**, *78*, 013810. [[CrossRef](#)]

15. Rudnicki, Ł.; Sánchez-Soto, L.L.; Leuchs, G.; Boyd, R.W. Fundamental quantum limits in ellipsometry. *Opt. Lett.* **2020**, *45*, 4607–4610. [[CrossRef](#)] [[PubMed](#)]
16. Machida, S.; Yamamoto, Y.; Itaya, Y. Observation of amplitude squeezing in a constant-current-driven semiconductor laser. *Phys. Rev. Lett.* **1987**, *58*, 1000. [[CrossRef](#)]
17. Wu, L.A.; Kimble, H.J.; Hall, J.L.; Wu, H. Generation of squeezed states by parametric down conversion. *Phys. Rev. Lett.* **1986**, *57*, 2520. [[CrossRef](#)]
18. Vahlbruch, H.; Mehmet, M.; Danzmann, K.; Schnabel, R. Detection of 15 dB squeezed states of light and their application for the absolute calibration of photoelectric quantum efficiency. *Phys. Rev. Lett.* **2016**, *117*, 110801. [[CrossRef](#)] [[PubMed](#)]
19. Sizmann, A.; Horowicz, R.J.; Wagner, G.; Leuchs, G. Observation of amplitude squeezing of the up-converted mode in second harmonic generation. *Opt. Commun.* **1990**, *80*, 138–142. [[CrossRef](#)]
20. Vahlbruch, H.; Mehmet, M.; Chelkowski, S.; Hage, B.; Franzen, A.; Lastzka, N.; Goßler, S.; Danzmann, K.; Schnabel, R. Observation of squeezed light with 10-dB quantum-noise reduction. *Phys. Rev. Lett.* **2008**, *100*, 033602. [[CrossRef](#)]
21. Mehmet, M.; Ast, S.; Eberle, T.; Steinlechner, S.; Vahlbruch, H.; Schnabel, R. Squeezed light at 1550 nm with a quantum noise reduction of 12.3 dB. *Opt. Express* **2011**, *19*, 25763–25772. [[CrossRef](#)]
22. Shelby, R.M.; Levenson, M.D.; Perlmutter, S.H.; DeVoe, R.G.; Walls, D.F. Broad-band parametric deamplification of quantum noise in an optical fiber. *Phys. Rev. Lett.* **1986**, *57*, 691. [[CrossRef](#)]
23. Corney, J.F.; Heersink, J.; Dong, R.; Josse, V.; Drummond, P.D.; Leuchs, G.; Andersen, U.L. Simulations and experiments on polarization squeezing in optical fiber. *Phys. Rev. A* **2008**, *78*, 023831. [[CrossRef](#)]
24. Fiorentino, M.; Sharping, J.E.; Kumar, P.; Porzio, A.; Windeler, R.S. Soliton squeezing in microstructure fiber. *Opt. Lett.* **2002**, *27*, 649–651. [[CrossRef](#)]
25. Fiorentino, M.; Sharping, J.E.; Kumar, P.; Levandovsky, D.; Vasilyev, M. Soliton squeezing in a Mach-Zehnder fiber interferometer. *Phys. Rev. A* **2001**, *64*, 031801. [[CrossRef](#)]
26. Dong, R.; Heersink, J.; Corney, J.F.; Drummond, P.D.; Andersen, U.L.; Leuchs, G. Experimental evidence for Raman-induced limits to efficient squeezing in optical fibers. *Opt. Lett.* **2008**, *33*, 116–118. [[CrossRef](#)]
27. Wang, E.; Verma, G.; Tinsley, J.N.; Poli, N.; Salvi, L. Method for the differential measurement of phase shifts induced by atoms in an optical ring cavity. *Phys. Rev. A* **2021**, *103*, 022609. [[CrossRef](#)]
28. Anashkina, E.A.; Andrianov, A.V.; Corney, J.F.; Leuchs, G. Chalcogenide fibers for Kerr squeezing. *Opt. Lett.* **2020**, *45*, 5299–5302. [[CrossRef](#)] [[PubMed](#)]
29. Bogatskaya, A.; Schegolev, A.; Klenov, N.; Popov, A. Generation of Coherent and Spatially Squeezed States of an Electromagnetic Beam in a Planar Inhomogeneous Dielectric Waveguide. *Photonics* **2019**, *6*, 84. [[CrossRef](#)]
30. Agrawal, G.P. *Nonlinear Fiber Optics*, 6th ed.; Elsevier: Amsterdam, The Netherlands, 2019.
31. Serena, P.; Meseguer, A.C.; Poli, F.; Bononi, A.; Antona, J.C. Scaling properties of guided acoustic-wave Brillouin scattering in single-mode fibers. *Opt. Express* **2021**, *29*, 15528–15540. [[CrossRef](#)] [[PubMed](#)]
32. Shelby, R.M.; Levenson, M.D.; Bayer, P.W. Guided acoustic-wave Brillouin scattering. *Phys. Rev. B* **1985**, *31*, 5244–5252. [[CrossRef](#)]
33. Andrianov, A.V.; Kalinin, N.A.; Anashkina, E.A.; Egorova, O.N.; Lipatov, D.S.; Kim, A.V.; Semjonov, S.L.; Litvak, A.G. Selective excitation and amplification of peak-power-scalable out-of-phase supermode in Yb-doped multicore fiber. *J. Light. Technol.* **2020**, *38*, 2464–2470. [[CrossRef](#)]
34. Lin, R.; Udalcovs, A.; Ozolins, O.; Pang, X.; Gan, L.; Tang, M.; Fu, S.; Popov, S.; da Silva, T.F.; Xavier, G.B.; et al. Telecommunication Compatibility Evaluation for Co-existing Quantum Key Distribution in Homogenous Multicore Fiber. *IEEE Access* **2020**, *8*, 78836–78846. [[CrossRef](#)]
35. Balakin, A.A.; Skobelev, S.A.; Anashkina, E.A.; Andrianov, A.V.; Litvak, A.G. Coherent propagation of laser beams in a small-sized system of weakly coupled optical light guides. *Phys. Rev. A* **2018**, *98*, 043857. [[CrossRef](#)]
36. Anashkina, E.A.; Andrianov, A.V. Design and Dispersion Control of Microstructured Multicore Tellurite Glass Fibers with In-Phase and Out-of-Phase Supermodes. *Photonics* **2021**, *8*, 113. [[CrossRef](#)]
37. Folkenberg, J.R.; Nielsen, M.D.; Mortensen, N.A.; Jakobsen, C.; Simonsen, H.R. Polarization maintaining large mode area photonic crystal fiber. *Opt. Express* **2004**, *12*, 956–960. [[CrossRef](#)]
38. Stone, J.M.; Yu, F.; Knight, J.C. Highly birefringent 98-core fiber. *Opt. Lett.* **2014**, *39*, 4568–4570. [[CrossRef](#)] [[PubMed](#)]
39. Mansuryan, T.; Rigaud, P.; Bouwmans, G.; Kermène, V.; Quiquempois, Y.; Desfarges-Berthelemot, A.; Armand, P.; Benoist, J.; Barthélémy, A. Spatially dispersive scheme for transmission and synthesis of femtosecond pulses through a multicore fiber. *Opt. Express* **2012**, *20*, 24769–24777. [[CrossRef](#)]
40. Drummond, P.D.; Corney, J.F. Quantum noise in optical fibers. I. Stochastic equations. *J. Opt. Soc. Am. B* **2001**, *18*, 139–152. [[CrossRef](#)]
41. Corney, J.F.; Drummond, P.D. Quantum noise in optical fibers. II. Raman jitter in soliton communications. *J. Opt. Soc. Am. B* **2001**, *18*, 153–161. [[CrossRef](#)]
42. Bonetti, J.; Hernandez, S.M.; Grosz, D.F. Master equation approach to propagation in nonlinear fibers. *Opt. Lett.* **2021**, *46*, 665–668. [[CrossRef](#)]
43. Kong, Q.; Ying, H.; Chen, X. Shortcuts to Adiabaticity for Optical Beam Propagation in Nonlinear Gradient Refractive-Index Media. *Entropy* **2020**, *22*, 673. [[CrossRef](#)] [[PubMed](#)]
44. Stolen, R.H.; Ippen, E.P. Raman gain in glass optical waveguides. *Appl. Phys. Lett.* **1937**, *22*, 276–278. [[CrossRef](#)]

-
45. Bachor, H.A.; Ralph, T.C.; Lucia, S.; Ralph, T.C. *A Guide to Experiments in Quantum Optics*; Wiley-vch: Weinheim, Germany, 2004.
 46. Kunz, L.; Paris, M.G.A.; Banaszek, K. Noisy propagation of coherent states in a lossy Kerr medium. *J. Opt. Soc. Am. B* **2018**, *35*, 214–222. [[CrossRef](#)]
 47. Corney, J.F.; Drummond, P.; Heersink, J.; Josse, V.; Leuchs, G.; Andersen, U.L. Many-Body Quantum Dynamics of Polarization Squeezing in Optical Fibers. *Phys. Rev. Lett.* **2006**, *97*, 023606. [[CrossRef](#)]
 48. Hirose, K.; Furumochi, H.; Tada, A.; Kannari, F. Photon Number Squeezing of Ultrabroadband Laser Pulses Generated by Microstructure Fibers. *Phys. Rev. Lett.* **2005**, *94*, 203601. [[CrossRef](#)] [[PubMed](#)]